Citation: Hirt, C. and E. Wildermann (2018), Reactivation of the Venezuelan vertical deflection data set from classical astrogeodetic observations, *Journal of South American Earth Sciences*, 85, 97-107, https://doi.org/10.1016/j.jsames.2018.05.003. **Data set access** via https://mediatum.ub.tum.de/1435994.

Reactivation of the Venezuelan vertical deflection data set from classical astrogeodetic observations

Christian Hirt[1], Eugen Wildermann[2]

[1] Institute for Astronomical and Physical Geodesy (IAPG) & Institute for Advanced Study, Technical University Munich, Arcisstr 21, 80333 Munich, Germany, c.hirt@tum.de

[2] Laboratorio de Geodesia Física y Satelital, Escuela de Ingeniería Geodésica, Facultad de Ingeniería, Universidad del Zulia, Núcleo Técnico Calle 69 c Av. Guajira, Maracaibo 4001, Venezuela, ewildermann@fing.luz.edu.ve

Highlights

- Astrogeodetic vertical deflections (observed geoid slopes) are rare in South America
- A classical vertical deflection dataset exists for Cordillera de Mérida (Venezuelan Andes)
- Transformation to current reference frames to be compatible with modern geo-products
- Deflections reach amplitudes of ~60 arc-seconds in this rugged mountain area
- RMS-agreement of 2 arc-seconds with predictions from GGMplus. Data freely available.

Abstract

Astrogeodetic vertical deflections (VDs) are gravity field functionals which are independent from any other field observation such as gravity accelerations from gravimetry or geoid undulations from GPS and geometric levelling. They may be useful for the validation of global geopotential models or height transfer via GPS and astronomical levelling. VDs are sensitive to the local mass-distribution, so can be used in geophysical studies, too. Over Southern Hemisphere continents in general and South America in particular, VDs are exceptionally rare. This paper describes the reactivation of a unique VD data set that extends over parts of the Andes Mountains in Venezuela. The VD data was acquired 1983 and 1985 with classical astrogeodetic instrumentation at 24 field stations along a ~80 km traverse crossing the Cordillera de Mérida with observation site elevations as high as ~4,500 m. To be compatible with modern geocentric gravity field products, the geodetic coordinates of the VD sites were transformed from the historic (non-geocentric) Venezuelan reference system to the geocentric ITRF2014, with residuals smaller than ~1 m. In the ITRF, the measured VDs have RMS signal strengths of ~20 arc-seconds (North-South) and ~14 arc-seconds (East-West), with magnitudes exceeding 60 arc-seconds at one benchmark. The observed VDs were compared against VDs from GRACE, GOCE and EGM2008 data and from the ultra-high resolution GGMplus gravity maps. The GGMplus model was found to capture ~85 to 90% (in terms of root-mean-square signals) of the measured VD signals. Both VD components are in ~2 arc-sec agreement with GGMplus. Overall, the agreement between observed VDs and modelled VDs is considered satisfactory, given the VDs were measured in a topographically rugged region, where residual signals may be large and global models are not well supported through regional terrestrial gravity data. The VDs may be useful, e.g., for the assessment of high-frequency constituents of present and future high-degree gravitational models (e.g., EGM2020) and calibration of model commission errors. The Venezuelan VD data is freely available.

Key words. Gravity field, vertical deflections, zenith camera, astrolabe, Venezuela, Andes, South America, ITRS, GGMplus

1 Introduction

Vertical deflections (VDs) are angular differences between the direction of the plumb line and some geometric reference direction. With the ellipsoidal normal as reference direction at the Earth's surface, VDs in Helmert definition are obtained (Jekeli 1999). Global Navigation Satellite Systems (GNSS), such as the Global Positioning System GPS (e.g., Seeber 2003) deliver geodetic coordinates that define the ellipsoidal normal. The direction of the plumb line can be determined with astrogeodetic instrumentation for star observation and precise timing equipment (e.g., Torge and Müller 2012, p162ff).

Before the advent of satellite surveying techniques, regional best-fitting ellipsoids were often used as reference for the geodetic coordinates. In that case, VDs are defined in a regional reference frame. Opposed to this, VDs are globally consistent when a global geocentric ellipsoid aligned to the axes of the International Terrestrial Reference System (ITRS) is used. When referred to a regional ellipsoid, VDs are sometimes denoted as *relative* VDs, and, conversely, in case of a global geocentric ellipsoid as *absolute* VDs (e.g., Featherstone and Rüeger 2000, Featherstone and Oliver 2013).

The primary value of astrogeodetic VDs is their independence from any other gravity field observable (e.g., gravity accelerations from gravimetry, gravity gradients from gradiometry, or geoid undulations from GPS heights and geometric levelling), making them suitable for validation of gravity field models (e.g., Jekeli 1999). As another benefit, astrogeodetic VDs can be used for economic transfer of height differences by combining the classical technique of astronomical levelling with GPS heighting (Hirt 2004). They are also suitable for geophysical study of the local mass-density distribution (e.g., Tugluoglo 1971, Wildermann 1988, Bürki 1989, Somieski 2008).

Historically, classical instrumentation such as theodolites or astrolabes were used for VD measurements. In the ~1970s, photographic zenith cameras were developed to accelerate the field observation (e.g., Wissel 1982, Wildermann 1988, Bürki 1989). Since the beginning of the 21st century, astrogeodetic observations are mostly carried out with efficient and automated digital instruments such as digital zenith cameras (e.g., Kudrys 2009, Hirt et al. 2010a; Abele et al. 2012, Halicioglu et al. 2012, Hanada et al. 2012, Wang et al. 2014, Guillaume 2015) or imaging theodolites (Guillaume et al. 2012, Tóth and Völgyesi 2016, Hauk et al. 2017, Schack et al. 2018).

Today, available VD data sets concentrate on North America (Pavlis et al. 2012, Smith et al. 2013, van Westrum 2016, Wang et al. 2017) and Europe (e.g., Bürki 1989, Kühtreiber 2003, Hirt 2004, Müller et al. 2004, Bürki et al. 2007, Somieski et al. 2007, Somieski 2008, Hirt et al. 2010b, Voigt 2013, Bucha et al. 2016), and also cover parts of Australia (Claessens et al. 2009, Schack et al. 2018). However, most countries of Asia, Africa and South America are still devoid of VD observations. An exception is Venezuela, where dedicated VD measurement campaigns have been carried out in 1983 and 1985 along a geo-traverse crossing the Merida Mountains (Wildermann 1988). The VD data has been collected with a photographic zenith camera and astrolabe at 24 field stations and utilized in a case study of the rugged gravity field of the Andes (Wildermann 1988).

The goal of the present paper is to reactivate the Venezuelan VD data set for modern gravity field studies. We start by giving a brief review of the VD campaigns and instrumentation deployed in the Merida Mountains (Section 2). Then, the transformation of the original geodetic station coordinates from the local network to the ITRS is described. This is crucially important to make the VDs compatible with modern gravity field data that implicitly relies on global geocentric reference frames (Section 3). The transformed VDs are then compared with VDs derived from two global gravity field models of different spatial resolution, showing relatively good agreement between both data sets (Section 4). Error sources affecting the quality of the VDs are discussed in Section 5 before an outlook is given in Section 6.

The VD data set discussed in this paper can be rated as exceptionally rare. To the knowledge of the authors, the Venezuelan VD data is one of the few – if not the only VD traverse data set – that is available over the Andes in particular and South America in general. The data set covers one of the topographically most rugged regions in the world, and extends over an elevation range of ~4500 m. Opposed to other parts of the world, terrestrial gravity data sets are not very dense over Venezuela. Consequently, global gravity field models are not very well supported by ground observations at short spatial scales, and VD data set might be valuable for model validation. Because of the current political situation of Venezuela, new VD measurements cannot be expected to be taken anytime soon over the Merida Mountains, underlining the importance of reactivating already existing data. Related to our work is a study by Featherstone and Olliver (2013) who reactivated a historic VD data set over Great Britain.

For readers not so familiar with general geodetic concepts and physical geodesy, we refer to the text book by Torge and Müller (2012). A focus on satellite geodetic concepts and coordinate frames is given by Seeber (2003). For an overview on astronomical geodesy, see, e.g., Torge and Müller (2012, Chapter 5.3). Applications for astrogeodetic vertical deflections are discussed, e.g., in Jekeli (1999), Hirt et al. (2010a) and Featherstone and Olliver (2013).

2 Field measurements

The purpose of this section is to give a brief account of the (historic) astrogeodetic field measurements, as documented in detail in Wildermann (1988). As study area, the central part of the Merida Mountains *(Cordillera de Mérida),* bounded by 8° and 10° Northern latitude and -72° to -70° Western longitude was chosen (Fig. 1). The Merida Mountains, located in the collision zone between the South American and Caribbean Plates (e.g., Gregory-Wodzicki 2000, Avé Lallemant and Sisson 2005) form the North-Eastern end of the Andes, and reach elevations of up to ~4,900 m. The geodetic network established for the astrogeodetic field measurements consists of 24 benchmarks (BMs) with ellipsoidal elevations from ~25 m to ~4,525 m. The main motivations of the geodetic field works by Wildermann (1988) were to establish an extended geodetic control network for a) deformation monitoring and b) determination of astrogeodetic VDs that enabled accurate physical heighting and study of local gravity field and mass-density structures. The geodetic control network (named “geotraverse”) begins near Lake Maracaibo (BM 33 in Fig. 1), widens over the High Andes network and ends near Ciudad Bolivia (BM 70), with a total length of ~80 km. The High Andes network covers an area of ~25 km x ~15 km in the North-Western and South-Eastern Mountain chains (highlighted in Fig. 1).

For the measurement of the direction of the plumb line (defined through the astronomical coordinates latitude Φ and longitude Λ), the transportable zenith camera TZK2 (Wissel 1982, Torge 2001, p161) by University of Hanover and an astrolabe (type Zeiss Ni2, cf. Torge and Müller 2012, p164) were available. The zenith camera TZK2 was deployed in February and March 1983 at 16 benchmarks, and the Ni2 in January to March 1983 and February 1985 at 11 benchmarks along the geotraverse (see Fig. 1).

- Zenith camera observations took place mostly in the Northern part of the Geotraverse (Fig. 1), where the equipment could be transported along mountain roads with a suitable all-terrain vehicle (Wildermann 1988, p22). Because of the semi-automated photographic star observation, up to 4 stations were observed per night. The AGK3 catalogue was used for the astrometric reduction of the photographs (Wildermann 1988, p18).

- Astrolabe observations were taken at field sites that were inaccessible for the zenith camera equipment, mostly in the central and Southern part of the traverse (Fig. 1). Depending on the site location, the comparatively light-weight equipment was moved by car, mules or even by foot (Wildermann 1988, p27), and mostly one station could be measured per night. Processing of the Ni2 observations relied on the FK4 star catalogue (Wildermann 1988, p18).

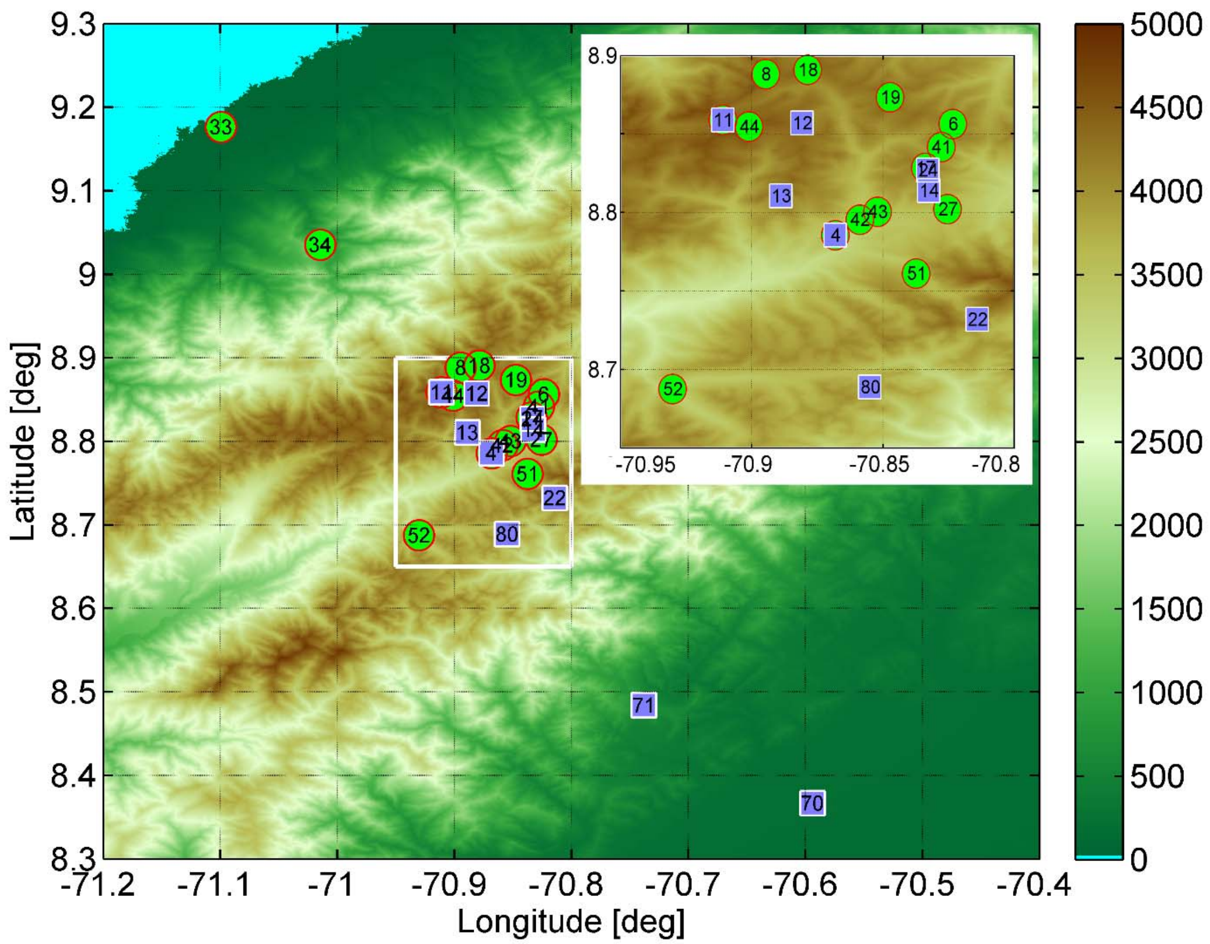

Fig.1 Topographic map of the North-Eastern extension of the Venezuelan Andes, known as *Cordillera de Mérida* (Merida Mountains), and location of the 16 zenith camera measurements (green circles, BM 4 and BM 11 observed with zenith camera, too) and 11 astrolabe measurements at 10 sites (blue squares). Topography from the MERIT DEM.

For time-tagging of all astrogeodetic observations, the YVTO time signal broadcasting service of Caracas, Venezuela, was used (satellite-based time tagging was not yet a mature technique back in 1983). The determination of geodetic coordinates (latitude φ, longitude λ) of the benchmarks was based on a combination of terrestrial network measurements (distances, angle measurements) mostly applied to connect the BMs in the central part of the traverse, and satellite Doppler measurements (e.g., Torge and Müller 2012, p131ff), linking 14 BMs across the entire traverse. The geodetic coordinates were adjusted with respect to the (non-geocentric) national terrestrial reference frame of Venezuela valid in 1983 (cf. details in Section 3.1).

3. Transformation of original network coordinates to ITRF2014

In principle, there are different avenues for obtaining the geodetic coordinates of the (historical) BMs in a current International Terrestrial Reference Frame (ITRF), such that absolute VDs can be computed:

- The first, ideal way is to transform the original network from a historical national reference system to ITRF via a set of identical points that are also coordinated in a geocentric system.
- The second option is to utilize Google Earth or similar platforms to measure BM coordinates directly in the digital imagery or vectorized maps (cf. Potere 2008 and Mohammed et al. 2013).. This, however, requires reliable knowledge to identify original observation sites (e.g., near road junctions). The accuracy of orthorectified satellite imagery needs to be considered over the highly mountainous terrain of the study area.
- The third option is to approach the transformation task as optimization problem, whereby gravity field residuals (between ITRF-transformed field observations and predictions from high-resolution models such as GGMplus, Hirt et al. 2013) are minimized as a function of the transformation parameters “regional system$\rightarrow$ITRF”. This idea conceptionally extends analyses of gravity field residuals done by Featherstone and Olliver (2013).
- As a forth option, height residuals between ITRF-transformed BM coordinates (latitude, longitude and height) and a sufficiently high-resolution digital elevation model (DEM) could be minimized in a similar way as gravity field residuals in the previous option.

In this study, the first option (use of identical points) is fortunately applicable for most stations and the second option (Google Earth) is used only at very few stations under specific topographic conditions and as an additional check. The other variants could be useful in the future for the re-activation of other historic gravity data sets without a sufficient number of identical points coordinated in historical and modern coordinate frames.

3.1 The original network

Designed mainly for geodetic analysis, deformation purposes and monitoring plate motions at the Caribbean South American tectonic plate boundary, the original first-epoch observations of the terrestrial network were only very loosely connected to the former Venezuelan national terrestrial reference frame (Provisional South American Datum of 1956, abbreviated to PSAD56) that is based on the Hayford ellipsoid (semi-major axis of 6,378,388 m and flattening of 1/297) and the fundamental point *La Canoa* ($\varphi = 8°\,34'17.17", \lambda = 296°\,8'\,25.12"$). In the sequel we use the acronym PSAD56-La Canoa as a synonym for the terrestrial reference frame used for the geo-traverse.

Recognizing the need of geodetic coordinates for all VD stations, efforts were made in 1985 to organize a dedicated Doppler-Transit satellite observation campaign in translocation mode with Canadian Marconi Transit Doppler equipment (Torge, 1985). Three points of the conventional terrestrial network were included. Beside the central network station at the astrophysical observatory (BM 4 in Fig. 1) one point situated in the northern network periphery (BM 8) and the third one in the eastern part, near the Mucubaji-Lagoon (BM 27) were occupied covering most of the local network and allowing the determination of Doppler-WGS72 geocentric coordinates for the whole local network. Back then, a three parameter transformation approach was applied, yielding three translations components between WGS72 minus the PSAD56-La Canoa (Table 1, middle column). This allowed the transformation of the geodetic coordinates from Doppler measurements in WGS72 to the PSAD56-La Canoa, such that the BMs of the entire network could be coordinated in the national reference system and *relative* VDs were obtained. Residuals after transformation at the three datum points were found at the ±10m level, approximately satisfying the requirements for VD determinations at the ±0.5" level in 1985 (Wildermann, 1988).

Table 1. Transformation parameters between Cartesian geocentric coordinates of the adjusted terrestrial network (PSAD56-La Canoa) and WGS72.

Parameter \ Transformation direction	PSAD56-La Canoa → WGS72 (Wildermann 1988)	PSAD56-La Canoa →WGS72 (this work)
dX	264.65 m	51.96 m
dY	– 113.28 m	201.08 m
dZ	371.80 m	-504.63 m
rotX	0.0	-0.8856D-03 [rad]
rotY	0.0	0.2487D-02[rad]
rotZ	0.0	-0.4593D-03[rad]
scale	1.0	1.0

3.2 New transformation

Considering the rather simplistic three-parameter connection between the original terrestrial network and WGS72, it was decided for this paper to re-adjust the geodetic network coordinates using not only translations, but also rotation components (rotX, rotY and rotZ). Because of the rather small network extension of ~30 km, the scale factor between WGS72 and terrestrial local coordinates is fixed to 1.0. This approach reduces the residuals well below the ±0.5 m level. Table 1 (right column) lists the transformation parameters that resulted from a re-adjustment using three identical points of the local geodetic network. The large differences (few 100 m amplitude) between the original and newly determined translation components reflect the local character of the network.

Applying the six transformation parameters in Table 1 (right column), all points of the local geodetic network were newly transformed to the geocentric WGS72-Doppler coordinate system. In the second step, these points - together with all other WGS72 translocation-Doppler stations observed in 1985 – were converted from WGS72 to WGS84 using the *National Geospatial-Intelligence Agency (NGA)* standardized transformation factors (NGA, 2014). Third, this approach was followed by applying the 7 parameter transformation from (ITRF, 2013) in an inverse ITRF90→WGS84 Doppler data transformation sense. Finally, an inverse 14 parameter ITRF2014→ITRF90 – transformation (ITRF, 2017) yielded coordinates compatible in the International Terrestrial Reference Frame 2014 (ITRF2014) valid today (cf. Altamimi et al. 2016).

The described multi-step transformation method was applied to convert geodetic coordinates (latitude φ, longitude λ, height *h*) of the 24 BMs of our network from the PSAD56-La Canoa (used in 1983-1985) to the (geocentric) ITRF2014. At the beginning and the end of the transformation chain, Helmert projections (as described in Torge and Müller 2012, p97) were applied to transform between the curvilinear geodetic and 3D Cartesian geocentric coordinates. Fig. 1 displays and Table 2 lists the geodetic coordinates of all 24 BMs in ITRF2014 together with the site names used in Wildermann (1988, p101).

Table 2. ITRF2014 geodetic coordinates of the 24 benchmarks (BMs) of the geotraverse "Merida Mountains". BM numbers and names correspond to Table 7.1 in Wildermann (1988)

BM Nr	BM name	Geodetic latitude [°]	Geodetic longitude [°]	Geodetic height [m]
4	Observatorio	8.78551491	289.13177818	3571.60
6	Antena	8.85632008	289.17657553	4258.92
8	Ventana Grande	8.88818814	289.10528139	4502.15
11	Cuenca Chama	8.85897669	289.08902705	4396.26
12	Punto Central	8.85710614	289.11912816	4457.59
13	Pico Observatorio	8.81044946	289.11107514	4352.59
14	Punta Colorada	8.81391240	289.16738913	4012.34
17	Aguila Nueva	8.82843863	289.16610775	4196.41
18	Ventana Pequena	8.89087047	289.12127961	4389.11
19	Puente	8.87349261	289.15259779	4379.25
22	Ventana Cruz Se	8.73196938	289.18582263	4157.52
24	Aguila Viejo	8.82689996	289.16701279	4142.54
27	Mucabaji	8.80210124	289.17454978	3592.32
33	Caja Seca	9.17655113	288.90063861	25.53
34	Torondoj	9.03554444	288.98531445	1108.17
41	Aguila Condor	8.84161827	289.17211960	4047.69
42	San Isidro	8.79546941	289.14111390	3327.49
43	Apartaderos	8.80053053	289.14786390	3422.03
44	Gregorio Paso	8.85461108	289.09895279	4524.99
51	Ventana Cruz Val	8.76103774	289.16261196	3584.93
52	Gavidia Pueblo	8.68759377	289.06976741	3245.63
70	Cuidad Bolivia	8.36693552	289.40603447	174.47
71	Catalina	8.48393136	289.26205668	645.34
80	Laguna Canoa	8.68884524	289.14499056	3793.07

After the transformation, the sets of geodetic coordinates (PSAD56-La Canoa from Wildermann 1988, Table 7.1 ibid, and ITRF2014 coordinates from Table 2) were compared. ITRF2014 latitudes are smaller than PSAD56-La Canoa latitudes. Depending on the location, latitude differences range between –11.24" and –12.18". Likewise, ITRF2014 longitudes are smaller too, with differences varying between –5.78" and –7.31", and ellipsoidal heights in both systems differing by ~5 m or less. Not surprising, this shows the direct dependence of VD components on the terrestrial reference frame (ellipsoid parameters and geodetic datum) the geodetic coordinates refer to. We note that for high-precision height transformation, the consideration of the so-called scale-induced indirect effect (Kotsakis 2008) may be relevant.

3.3 Verification

Fortunately, one of the BMs, BM 41, occupied with the zenith camera has been included into the current national fundamental SIRGAS/REGVEN (*Sistema de Referencia Geocéntrico para América del Sur - Red Geodésica Venezolana*) GPS network, named officially *Pico El Aguila* (IGVSB, 2017a), along with the central network point, BM 4, named now officially *Observatorio* (IGVSB, 2017b). Defined in SIRGAS/REGVEN, only one transformation into ITRF2014 is needed. Comparing at *Observatorio* the transformed coordinates, originally coming from the Doppler-technique approach, with these new GPS network values, differences in latitude of +0.149" (about 4.6 m) and in longitude of –0.204" (about 6.3 m) were obtained. These indicate that the geodetic coordinates of the BMs – coordinated in ITRF2014 – are accurate to few 0.1".
As another plausibility check on the BM coordinates, we compared the ITRF2014 geodetic heights of the 24 BMs with those interpolated from a high-resolution digital elevation model (DEM). As DEM, the 3 arc-sec resolution MERIT (Multi-Error Reduced Improved Terrain) DEM by Yamazaki et al. (2017) and the 1 arc-sec resolution SRTM v3 model by NASA (NASA, 2017) were used which are primarily based on data from the Shuttle Radar Topography Mission (SRTM), cf. Farr et al. (2007). The EGM96 geoid model (the SRTM height reference surface) was subtracted from the DEM to yield geodetic heights that can be compared with the ITRF2014 geodetic heights of our BMs. The differences between the ITRF station heights and DEM heights range between -14.8 m and +44.3 m, with a RMS (root-mean-square) agreement of 17.7 m. When the 1-arcsecond resolution SRTM v3 model by NASA is used, the agreement improves – because of the higher DEM resolution and better representation of terrain features – to 13.5 m RMS (min = -14.4 m and max =30.8 m). Over our rugged test area, large residuals (e.g., several 100 m) would have indicated a mismatch between the DEM-modelled topography and the 3D geodetic coordinates (particularly when there were remaining shifts in latitude and longitude, virtually moving the BM away from the DEM 3D surface), but are not observed here. This provides additional evidence of the ITRF2014 coordinates being plausible. We note that similar DEM comparisons might provide a useful check on the transformation of other gravity field data sets from historic to modern reference frames.

Mainly due to logistical reasons, only 4 original astronomical observation stations (BMs 22, 41, 42 and 43) have neither been incorporated in the terrestrial network 1983, nor included in the 1985 Doppler measurements campaigns. In the original calculations in the 1980s, their geodetic coordinate estimations have been based on well-defined topographic details identified in official Venezuelan topographic maps. Fortunately, all four BMs could be well identified in Google Earth (mountain crest (BM 22), road junctions (BMs 42 and 43) or visible monument (BM 41). The last site has become part of the SIRGAS-REGVEN GPS reference network in 1988 A direct check of these official coordinates (transferred to ITRF2014) with the estimated coordinates from Google Earth shows differences less than 0.2" at this high mountain station. The transformed official BM 41 GPS coordinates are reported in Table 2; only the remaining three sites have been located by Google Earth estimates.

4. Results and comparisons

The key result of this paper are the vertical deflections (VDs) computed from the original astronomical coordinates (latitude Φ and longitude Λ) and the ITRF2014 geodetic coordinates (latitude φ, longitude λ) listed in Table 2 for the 24 BMs. The North-South VD component ξ and East-West VD component η are obtained via the rigorous equations (Voigt 2013, p27)

$$\xi = \sin\Phi\cos\varphi - \cos\Phi\sin\varphi\cos(\Lambda - \lambda),$$
$$\eta = \sin(\Lambda - \lambda)\cos\Phi, \quad (1)$$

which are preferred here over the somewhat less accurate linear approximations (cf. Torge and Müller 2012, p228). The VDs observed with the TZK2 zenith camera are reported in Table 3 and the VDs observed with the Ni2 astrolabe in Table 4. While VDs computed from the (historic) PSAD56-La Canoa geodetic coordinates (cf. Wildermann 1988) are *relative*, the VDs reported in Table 3 and 4 are *absolute* because of the geocentric ITRF2014 used for the geodetic coordinates. The absolute VDs can be used for comparisons with VDs from geocentric gravity models (cf. Featherstone and Olliver 2013). Table 3 and 4 show large variations of our (absolute) VDs, with maximum xi-values reaching ~55" (BM 34) and eta values as large as ~40" (BM 71). The total VD

$$\theta = \sqrt{\xi^2 + \eta^2} \quad (2)$$

exceeds a magnitude of ~63" for BM 34 that is located at the Northern slope at the Merida Mountains. Some stations were occupied both with the TZK2 and the Ni2. For BM 4, the ξ differences are 1.40" and η-differences 0.15". For BM 11, the differences are 0.33" in component ξ and 1.50" in η between the two instruments (cf. Tables 3 and 4), cautiously suggesting a precision at the 1"-level. Further multiple occupations of the same BMs were not possible during the original campaigns.

Table 3. Vertical deflections at 16 BMs observed with the TZK2 zenith camera. Astronomical coordinates from Wildermann (1988, p25 ibid). For the ITRF2014 geodetic coordinates used to compute the VDs see Table 2

BM Nr	Astronomical latitude [°]	Astronomical longitude [°]	VD xi ["]	VD eta ["]
4	8.7865389	289.1321444	3.69	1.30
6	8.8604417	289.1781250	14.84	5.51
8	8.8972917	289.1018111	32.77	-12.34
11	8.8669944	289.0855750	29.28	-11.95
17	8.8311861	289.1684389	9.89	8.29
18	8.8987778	289.1183694	28.47	-10.35
19	8.8798944	289.1517500	23.05	-3.02
27	8.8039611	289.1768500	6.70	8.18
33	9.1856861	288.8948917	32.89	-20.42
34	9.0508028	288.9762917	54.93	-32.08
41	8.8444667	289.1742833	10.25	7.70
42	8.7970361	289.1414250	5.64	1.11
43	8.8016583	289.1477722	4.06	-0.33
44	8.8612639	289.0963806	23.95	-9.15
51	8.7633083	289.1633306	8.17	2.56
52	8.6901472	289.0679750	9.19	-6.38

Table 4. Vertical deflections at 10 BMs observed with the Ni2 astrolabe. Astronomical coordinates from Wildermann (1988, p34-35 ibid). For the ITRF2014 geodetic coordinates used to compute the VDs see Table 2

BM Nr	Astronomical latitude [°]	Astronomical longitude [°]	VD xi [“]	VD eta [“]
4	8.7869278	289.1321000	5.09	1.14
4	8.7865917	289.1321444	3.88	1.30
11	8.8669028	289.0851528	28.95	-13.45
12	8.8636194	289.1184972	23.45	-2.24
13	8.8126556	289.1100250	7.94	-3.74
14	8.8155194	289.1692833	5.79	6.74
22	8.7290611	289.1912139	-10.47	19.18
24	8.8292667	289.1687139	8.52	6.05
70	8.3641389	289.4106889	-10.07	16.58
71	8.4772500	289.2733111	-24.05	40.07
80	8.6864556	289.1502167	-8.60	18.60

Table 5. Descriptive statistics of the observed and modelled VDs and their differences at 24 BMs (multiple astronomical observations were averaged), unit in arc-seconds

Component		Min	Max	Mean	RMS
Xi	Observed	-24.05	54.93	12.11	20.62
	GGE	-26.76	51.70	11.50	20.05
	GGMplus	-24.47	53.79	10.77	20.04
	Observed – GGE	-2.98	8.63	0.61	2.53
	Observed – GGMplus	-1.79	3.76	1.34	2.03
Eta	Observed	-32.08	40.07	1.24	14.31
	GGE	-38.58	36.69	1.82	14.91
	GGMplus	-31.98	36.21	2.38	14.42
	Observed – GGE	-6.67	6.50	-0.58	2.78
	Observed – GGMplus	-3.32	3.86	-1.14	2.05

We have compared the astrogeodetic VDs from TZK and Ni2 observations with VDs from global gravity field models that represent gravity field information based on one or more of the three sources a) satellite gravity measurements from the GRACE and GOCE missions, b) terrestrial gravimetry and c) topographic mass models (DEMs together with mass-density assumptions). The models are:

1) The GGE (GRACE-GOCE-EGM2008) model, a combination of the Earth Gravitational Model EGM2008 (Pavlis et al. 2008, 2012, 2013) with satellite gravity data from the GRACE and GOCE missions (e.g., Pail et al. 2010) at long and medium wavelengths (see Hirt et al. 2013 for full details).
2) The GGMplus plus model (see Hirt et al. 2013) that augments model 1) at spatial scales of 10 km to ~220 m with short-scale VD information predicted from the SRTM topography (Hirt et al. 2014).

Fig 2 shows high-resolution VD maps over our study area based on these two models. VDs from model 1) have a spectral field resolution of ~20,000 km to ~10 km (or spherical harmonic degree 2190), while VDs from model 2) take into account gravity field structures at spatial scales of ~20,000 km to ~220 m. In both comparisons, VDs from the models are in Helmert definition (cf. Jekeli 1999; Torge and Müller 2012), which is consistent with the astrogeodetic observations. The Helmert definition was realised by applying two corrections to the VD component ξ (to account for the curvature of the normal plumb line and the ellipsoidal effect) computed from the model coefficients, as described in Hirt et al. (2010b, Eqs. 5-8 ibid). Over our study area, the plumb line correction does not exceed values of 0.25”, and the correction for the ellipsoidal effect remains below 0.1”.

Table 5 reports the descriptive statistics for the VDs from the astrogeodetic observations, from the two models, and the differences between observed and modelled VDs. For this comparison, the VD observations from the two instruments at BM 4 and at BM 11 were averaged, avoiding multiple VD values at identical BMs. It is seen that observed and modelled VDs have similar signal strengths (RMS of ~20.0 to 20.6” for ξ and ~14.3” to 15.0” for η, at the 24 BMs. The agreement between observed and modelled VDs is found to be at the RMS-level of ~2.5” (ξ) and 2.8” (η), when the spectral model resolution limited 10 km (GGE model).

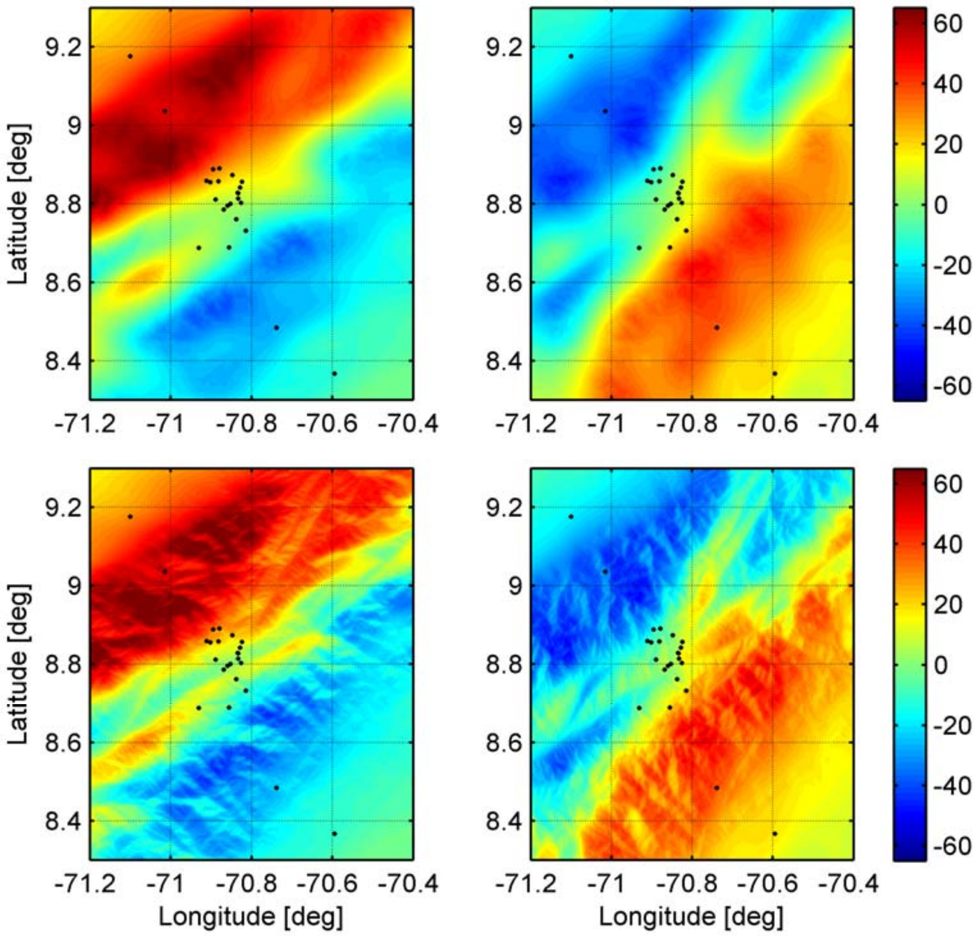

Fig.2. Modelled VDs over the study area together with the locations of observed VDs. Left column: North-South component ξ, right column: East-West component η, top row: VDs with ~10km spatial resolution (from GRACE/GOCE/EGM2008), bottom row: VDs with ~220 m resolution (from GGMplus).

The increase in spatial resolution from top to bottom due to using predictions based on topographic mass models is visible. Unit in arc-seconds

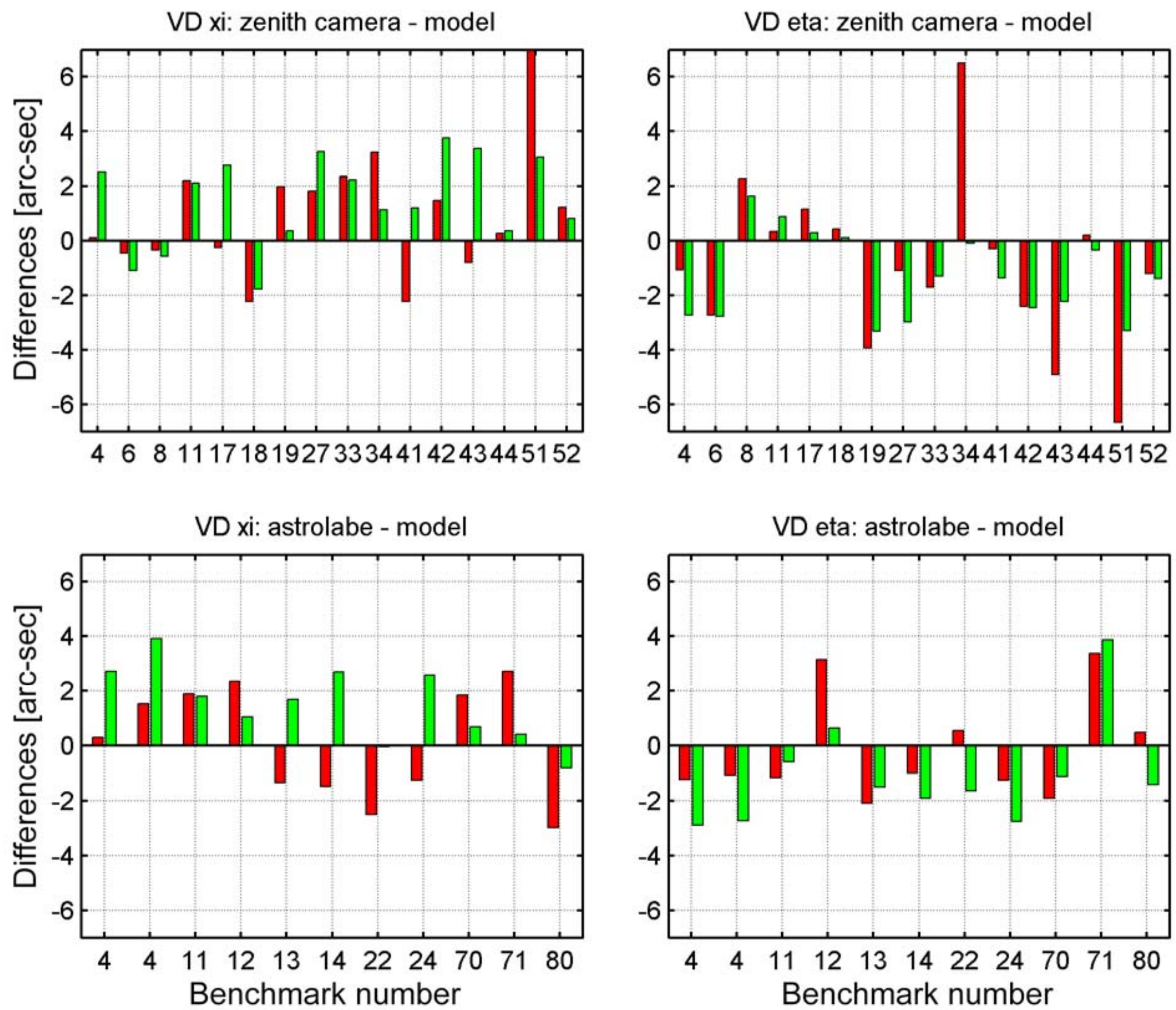

Fig.3 Differences between astrogeodetic VDs and modelled VDs, left column: North-South component ξ, right column: East-West component η, top row: VDs from zenith camera observations, bottom row: VDs from astrolabe observations. Differences in red refer to the GRACE/GOCE/EGM2008 model (resolution of 10 km), green differences refer to the GGMplus model (resolution of ~220 m). Unit in arc-seconds.

The RMS agreement is improved to the level of ~2.0” for both components, when the model resolution is extended to ~220 m (GGMplus), cf. Table 5. This translates into a reduction of RMS of ~25% (ξ) and ~35% (η) through inclusion of short-scale information from topographic mass models at scales of ~10 km to ~220 m. In terms of RMS signal strengths, the GGMplus model explains ~90% of measured VD signals in North-South direction and ~86% in East-West direction.

A comparison between VDs measured with the TZK2 zenith camera at 16 BMs (Table 3) shows an RMS agreement with GGMplus of 2.19” (ξ) and 2.04” (η); a similar comparison between the VDs measured at 10 BMs with the Ni2 astrolabe (Table 4) and GGMplus yields RMS values of 2.02” (ξ) and 2.15” (η). This comparison suggests that VDs from both instruments are of similar precision.

For all stations, Fig. 3 compares the residuals between observations and the two models GGE (red bars) and GGMplus (green bars) for the zenith camera sites (top row) and astrolabe sites (bottom row). The comparison show better agreement when a high-resolution model like GGMplus is used that is capable of representing short-scale VD variations associated with the local topographic masses. However, Fig. 3 also suggests the possible presence of remaining systematic errors in either the modelled or observed VDs, at the level of ~1” in both components (cf. mean values of the differences in Table 4).

5. Discussion

The geodetic coordinates of a classical VD data set have been transformed from the (historic) non-geocentric Venezuelan PSAD56-La Canoa to the geocentric ITRF2014, changing the geodetic latitudes by ~330-360 m (11”-12”) and ~180-200 m (6-7”), cf. Section 3. As a result, the VDs observed at 24 BMs with classical instrumentation could be computed with respect to ITRF, cf. Section 4. The VDs were found to agree at the RMS level of 2” with those from the currently highest-resolution global VD model, and up to 90% of observed VD signals is explained through the model. Overall, the agreement of the observed VDs with independent VDs from the GGMplus model is considered satisfactory, given the extreme topography of the test area and a number of limitations affecting both to the modelled and observed VDs.

5.1 Limitations of the observations

The observational precision of the Venezuelan VDs was assessed to be at the level of ~0.5-1.0”, both for the zenith camera (Wildermann 1988, p25) and the astrolabe observations (Wildermann 1988, p34). The transformation of geodetic coordinates from PSAD56-La Canoa to the geocentric ITRF2014 could contain uncertainties at the level of few 0.1”, as is indicated by comparisons with independent BMs (see Section 3.3). The Venezuelan VD observations took place between 1983 and 1985, well before the era of high-precision star catalogues from dedicated astrometry satellite missions. Such star catalogues provide star positions with 1/1000 arc-sec accuracies in case of the HIPPARCOS satellite (ESA 1997), or even better in case of the GAIA mission (Brown et al. 2016). Specifically, the star catalogues available for processing the zenith camera (AGK3 catalogue) and astrolabe observations (FK4) may contain errors of a few 0.1” (Wildermann 1988 p17ff). Unfortunately, the original observation records are not available anymore. These would have enabled a post-analysis of the star catalogue error for the specific stars used for the astronomic reductions (e.g. through comparisons with HIPPARCOS star positions) and possibly the computation of small corrections to refer the observed latitude Φ and longitude Λ to the ICRS (International Celestial Reference System), as realised through HIPPARCOS.

The zenith camera observations mostly took place at sites near roads, eccentric to the actual BMs of the local geodetic network. The geometric differences (offsets) $\Delta\varphi$ and $\Delta\lambda$ between the observation sites and BMs (often few 10s of meters) were applied as corrections to the (Φ, Λ) coordinates [as listed in Table 3] in Wildermann (1988). This implicitly assumed that the VDs of the eccentric astrogeodetic observation site and the actual BM are identical. However, particularly in rugged mountainous terrain, the horizontal gradients of VDs can reach or even exceed values of 1-2” per 100 m, as is seen in Fig. 4.

Because the horizontal gradients were not modelled, they act as additional error source affecting the VDs from zenith camera observations reported in Table 3.

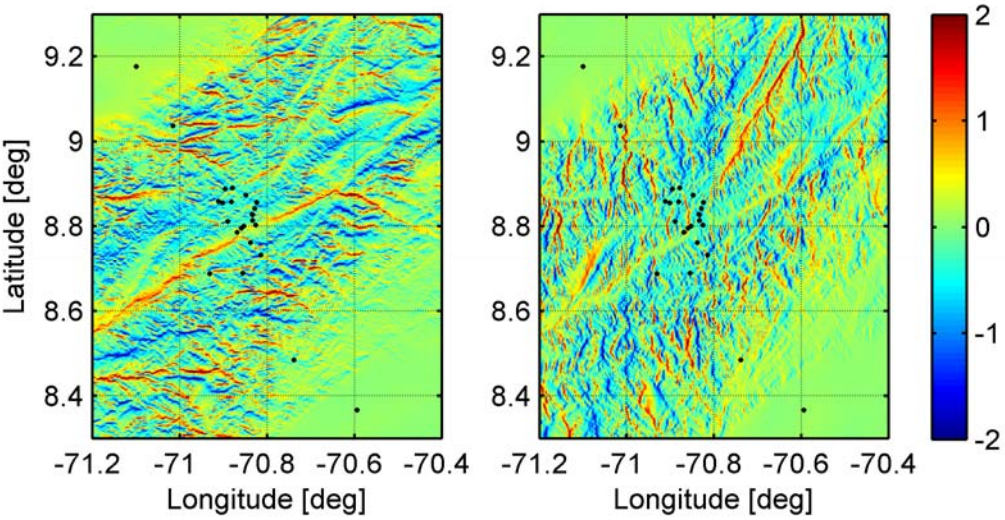

Fig.4. Horizontal VD gradients over the study area from GGMplus, left column: North-South gradient of the North-South component ξ, right column: East-West gradient of the East-West component η. VD gradients were formed numerically between adjoining GGMplus grid points, unit in arc-sec per 100 m. North-South gradients of η and East-West gradients of ξ are not shown.

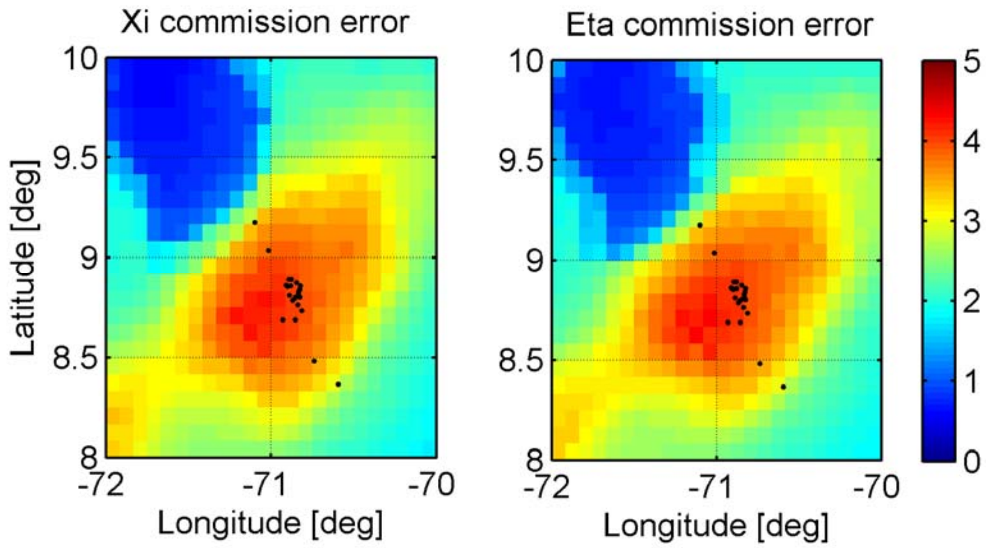

Fig. 5. EGM2008 commission (= model) error for VD components ξ (left panel) and η (right panel) over the Merida Mountains, together with the BMs of the geotraverse. Data from Pavlis et al. (2012), unit in arc-seconds

An attempt has been made to work out the horizontal offsets between the centric geodetic BMs (cf. Tab. 2) and the original astrogeodetic observation sites (eccentric to the geodetic BMs). From a comparison between centric and eccentric astronomical coordinates (cf. Table 2.5 in Wildermann 1988 and Appendix to Chapter 2 of Wildermann 1988) horizontal offsets $\Delta\varphi$ and $\Delta\lambda$ between centres and excentres have been deduced for the 16 TZK sites. As a test, we applied the offsets both to the geodetic coordinates (Table 2) and astronomical coordinates (Table 3) and compared the VDs with GGMplus, giving slightly improved RMS agreement of 2.09" (ξ) and 2.02" (η), for the 16 TZK stations [instead of 2.19" (ξ) and 2.04" (η)]. The horizontal offsets $\Delta\varphi$ and $\Delta\lambda$ are documented in Table 6.

5.2 Limitations of the models

Over Venezuela, the EGM2008 model (and, thus, GGMplus) is not as well supported by terrestrial gravity observations at spatial scales of ~120 km to ~10 km, as over, e.g., Europe, Australia and North America (cf. Pavlis et al. 2008, 2012, 2013). As a result of the poorer model support through gravity observations, the propagated uncertainty (also known as model commission error) associated with the full EGM2008 band-width reaches amplitudes of 4" over the Merida Mountains test area (Fig. 5). For comparison purposes, the EGM2008 VD commission error is at the level of ~0.5" over flatter parts of well-surveyed areas of Australia, Europe and North America, and increases to ~1" over mountainous areas of these continents. While the uncertainty estimate shown in Fig. 5 is somewhat reduced through the use of GOCE gravimetry (instead of EGM2008 information at spatial scales of ~80 to ~120 km) in GGMplus, it is reasonable to consider the terrestrial gravity data basis as one of the key factors limiting the model accuracy to few arc-seconds. Because of the classified nature of gravity data used in EGM2008 over large parts of South America (cf. Pavlis et al. 2012, 2013), it is not possible for us to investigate the density and quality of the Venezuelan gravity data that were used in EGM2008.

It is important to note that no gravity observations were used to support the modelled VDs at short scales (10 km) Instead, the high-frequency VD signal constituents in GGMplus are solely based on predictions using topographic models together with mass-density assumptions, and further simplifications (cf. Hirt et al. 2014). Over areas with pronounced sub-surface mass-density contrasts, it is entirely possible that the constant mass-density assumption of 2670 kg m^{-3} (that the GGMplus short-scale signal relies on) produces local model errors of up to 2-3" (e.g., Schack et al. 2018). While the predicted high-frequency component of GGMplus (spatial scales of ~10 km to ~220 m) was shown to substantially improve the agreement with the observed VDs (compare variants "Observed – GGE" and "Observed – GGMplus" in Table 5), there is also the effect of omitted ultra-short scale signals. The limited resolution of the topography model (here ~220 m) is not capable of representing ultra-short scale VD variations that might be captured in the VD observations, producing further model errors at the level of few ~0.1".

6 Conclusions and outlook

A rare VD data set, acquired in the Merida Mountains between 1983 and 1985 with classical analogue astrogeodetic instrumentation, has been re-activated. This has been achieved by transforming the geodetic coordinates from the historical (non-geocentric) Venezuelan reference frame to the geocentric ITRF2014 that is sufficiently compatible with modern geodetic products such as elevation or gravity field models. The VDs, referred to ITRF2014, have been found to be in ~2" RMS agreement with VDs from highest resolution global VD models (GGMplus).

In comparison to other VD data sets, e.g. over Europe, Australia and North America (where astrogeodetic observations and VDs predicted from GGMplus agree between ~0.5" and 1.1" in a RMS sense, cf. Hirt et al. 2013), the agreement is lower for our data set. A number of factors have been discussed in Section 5 that may contribute to the observed discrepancies. The rather poor support of global models through terrestrial gravity data sets is considered one of the key contributors limiting the agreement between modelled and observed VDs. Notwithstanding, the comparisons give – for the first time – evidence that even over highly mountainous terrain and one of the "EGM2008 problem areas" (areas devoid of dense terrestrial gravity data sets) the GGMplus model may be capable of predicting VDs at a precision level of 2". The comparisons may suggest that the EGM2008 commission errors (4" over the Merida Mountains, cf. Pavlis et al. 2012) are too pessimistic over Venezuela. The

VDs may therefore be useful to calibrate the commission error estimates accompanying future high-degree geopotential models such as EGM2020 (Barnes et al. 2015). As another follow-up work, the Venezuelan VDs could be used for geophysical study of the mass-density structure of the Merida mountains, together with modern data sets from satellite observations (e.g., gravity from the GOCE mission, Pail et al. 2010, and topography from SRTM, Farr et al. 2007).

The re-activated Venezuela VD data set is – to the knowledge of the authors – one of the few, if not the only astrogeodetic data set that exists in the Andes mountains in particular, and South America in general. Despite the rather small number of stations, the VD data set might be of value to gauge over one of the topographically roughest areas of South America improvements associated with future gravity models, coming specifically with the development of EGM2020, or successor models to GGMplus. Because of the traverse length of ~80 km, and station concentration on a local ~25 km x ~15 km area (Fig. 1), the data set is expected to be useful in sensing the short-scale model performance at or below scales of few 10s of km. Opposed to this, the suitability for testing satellite gravity data sets is expected to be rather limited because of the ~100 km resolution level associated with satellite gravimetry.

Together with two VD data sets available over Australia (Schack et al. 2018, Claessens et al. 2009) and the Venezuelan VDs described in this paper, there are now three VD data sets available "outside" Europe and North America that have been recently deployed in validation studies. One of the key benefits of VD data sets is their independence from other gravity field products and their sensitivity to short-scale gravity field variations, making them an important data source for testing gravity field products.

Compared to GPS/levelling data sets, VDs play a complementary role for gravity field validation (Hirt et al. 2010b). This is firstly because VDs are particularly sensitive for short-wavelength field constituents. Secondly, without the need to perform geometric levelling, as in case of GPS/levelling data, VDs can be measured today relatively easily even along traverses with large elevation differences (e.g., few 1000 m, as in the Merida Mountains). Further extension of the scarce VD data base on Southern Hemisphere continents would be desirable to improve testing capabilities for current and future gravity field products.

As future work, dedicated VD campaigns, e.g. along ~200-400 km long traverses crossing the Chilean, Peruvian or Ecuadorian Andes should be considered, deploying state-of-the-art astrogeodetic instrumentation such as digital zenith cameras (Hirt et al. 2010) or digital imaging tachymeters (Guillaume et al. 2012, Guillaume 2015, Hauk et al. 2017). Particularly light-weight imaging tachymeters appear promising for such field projects because they can be easily shipped by plane and transported along mountain roads. An accuracy of ~0.2" for the VD components can be expected (cf. Hauk et al. 2017). Besides the higher observational accuracy, all other limitations described in Sect. 5.1 (remaining uncertainties associated with the star catalogue, geodetic coordinates, station centering as described in Section 5 for the reactivated Venezuelan VD data) can be avoided, thereby increasing the testing power of the VDs for gravity field model validation and error calibration.

Acknowledgements Both authors would like to thank Prof. Günter Seeber who inspired and (co)-supervised their PhD studies in different decades (1983-1988 and 2001-2004). CH would like to acknowledge support by the German Research Foundation (grant Hi 1760/01). EW would like to thank Stiftung Volkswagenwerk for supporting field work for the 1983-1985 observations and Prof. Wolfgang Torge as principal supervisor of his PhD thesis.

Data statement Following the philosophy of open science, the data set described in this study is freely available for research and education, and a further contribution towards an unrestricted global VD data base (also see Schack et al. 2018). The VD data file is available via https://mediatum.ub.tum.de/1435994.

Table 6. Horizontal offsets $\Delta\varphi$ (in North-South direction) and $\Delta\lambda$ in East-West direction between the geodetic BM coordinates and original (eccentric) zenith camera sites in arc-seconds. Note that the reported offsets are implicitly included in the astronomical coordinates reported in Table 3. When the offsets are added to the astronomical coordinates in Table 3, the Φ and Λ values originally observed at the eccentric camera site are obtained.

BM	$\Delta\varphi$ [“]	$\Delta\lambda$ [“]
4	3.70	-0.99
6	-0.93	-2.78
8	0.52	3.96
11	0.00	0.00
17	5.83	6.44
18	0.94	0.76
19	-0.95	0.75
27	0.36	1.16
33	-1.20	-0.17
34	1.01	-0.66
41	1.20	0.17
42	-0.79	-0.92
43	-1.10	0.50
44	-0.78	0.93
51	-1.21	0.11
52	1.21	-0.05

References

Abele, M., Balodis., J, Janpaule, I., Lasmane, I., Rubans, A., Zarinš., A. 2012. Digital zenith camera for vertical deflection determination, Geod. and Cart., 38 (4), 123-129.

Altamimi, Z., Rebischung, P., Métivier, L., Collilieux, X., 2016. ITRF2014: A new release of the International Terrestrial Reference Frame modeling nonlinear station motions. J. Geophys. Res. Solid Earth 121, 6109–6131.

Avé Lallemant, H.G., Sisson, V.B., 2005. Caribbean-South American plate interactions, Venezuela. Geological Society of America, doi:10.1130/SPE394 ISBN (print): 9780813723945.

Barnes, D., Factor, J.K., Holmes, S.A., Ingalls, S., Presicci, M.R., Beale J., Fecher, T., 2015. Earth Gravitational Model 2020, presented at American Geophysical Union, Fall Meeting 2015, abstract id. G34A-03, Available at: http://adsabs.harvard.edu/abs/2015AGUFM.G34A..03.

Brown, A.G.A., et al., 2016. Gaia Data Release 1, Summary of the astrometric, photometric, and survey properties, Astron. Astrophys. 595, A2, doi:10.1051/0004-6361/201629512

Bucha, B., Janak, J., Papco, J., Bezdek, A., 2016. High-resolution regional gravity field modelling in a mountainous area from terrestrial gravity data. Geophys. J. Int. 207, 949–966.

Bürki, B., 1989. Integrale Schwerefeldbestimmung in der Ivrea-Zone und deren geophysikalische Interpretation. Geodätisch-geophysikalische Arbeiten in der Schweiz, Nr. 40, Schweizerische Geodätische Kommission.

Bürki, B., Somieski, A.E., Sorber, P., Kahle, H.-G., Hirt, C. 2007. The Digital Astronomical Deflection Measuring System (DIADEM), In: Swiss National Report on the Geodetic Activities in the years 2003-2007, presented to the XXIV General Assembly of the IUGG in Perugia, Italy, ISBN 978-3-908440-15-4, Swiss Geodetic Commission, 143-144.

Claessens S.J., Featherstone, W.E., Anjasmara, I.M., Filmer, M.S., 2009. Is Australian data really validating EGM2008 or is EGM2008 just in/validating Australian data. In: Newton's Bulletin (2009), 207-251.

ESA (1997). The Hipparcos and Tycho Catalogues. ESA SP-1200.

Farr, T.G., Rosen P.A., Caro E., Crippen R., Duren R., Hensley S., Kobrick M., Paller M., Rodriguez E., Roth L., Seal D., Shaffer S., Shimada J., Umland J., Werner M., Oskin M., Burbank D., Alsdorf D. 2007. The Shuttle Radar Topography Mission. Rev. Geophys. 45, RG2004.

Featherstone, W. E., Rüeger, J. M., 2000. The importance of using deviations of the vertical in the reduction of terrestrial survey data to a geocentric datum. The Trans-Tasman Surveyor 1 (3), 46-61. [Erratum in The Australian Surveyor 47(1): 7]

Featherstone, W. E., Olliver, J. G., 2013. Assessment of EGM2008 over Britain using vertical deflections, and problems with historical data. Survey Review 45 (332), 319-324.

Gregory-Wodzicki, K.M. 2000. Uplift history of the Central and Northern Andes: A review The Geological Society of America (GSA) Bulletin 112 (7), 1091–1105.

Guillaume, S., Bürki, B., Griffet, S., Mainaud-Durand, H., 2012. QDaedalus: Augmentation of total stations by CCD sensor for automated contactless high-precision metrology. FIG Proceedings 2012, https://www.fig.net/resources/proceedings/fig_proceedings/fig2012/papers/ts09i/TS09I_guillaume_buerki_et_al_6002.pdf

Guillaume, S., 2015. Determination of a Precise Gravity Field for the CLIC Feasibility Studies. Dissertation Nr. 22590, Eidgenössische Technische Hochschule ETH Zürich, Switzerland. doi: 10.3929/ethz-a-010549038.

Halicioglu, K., Deniz, R., Ozener, H., 2012. Digital zenith camera system for Astro-Geodetic applications in Turkey. J. Geod. and Geoinf. 1 (2), 115-120.

Hanada, H., Araki, H., Tazawa, S., et al., 2012. Development of a digital zenith telescope for advanced astrometry, Science China Physics, Mechanics & Astronomy 5 (4), 723-732.

Hauk, M., Hirt, C., Ackermann, C., 2017. Experiences with the QDaedalus system for astrogeodetic determination of deflections of the vertical. Survey Review 49 (355), 294-301.

Hirt, C., 2004. Entwicklung und Erprobung eines digitalen Zenitkamerasystems für die hochpräzise Lotabweichungsbestimmung. Wissen. Arb. der Fachrichtung Geodäsie und Geoinformatik an der Universität Hannover Nr. 253.

Hirt C., Bürki, B., Somieski, A., Seeber, G., 2010a. Modern Determination of vertical deflections using digital zenith cameras. J. Surv. Eng. 136(1), 1-12.

Hirt C., Marti U., Bürki B. and Featherstone W.E., 2010b. Assessment of EGM2008 in Europe using accurate astrogeodetic vertical deflections and omission error estimates from SRTM/DTM2006.0 residual terrain model data. J. Geophys. Res. – Solid Earth, Vol. 115, B10404.

Hirt, C., Claessens, S.J., Fecher, T., Kuhn, M., Pail, R., Rexer, M., 2013. New ultra-high resolution picture of Earth's gravity field. Geophys. Res. Lett. 40, doi: 10.1002/grl.50838.

Hirt C., Kuhn, M., Claessens, S.J., Pail, R., Seitz, K., Gruber T., 2014. Study of the Earth's short-scale gravity field using the ERTM2160 gravity model. Comp. Geosci. 73, 71-80.

IGVSB, 2017a. Instituto Geográfico de Venezuela Simón Bolívar, Estado MERIDA, Vertice Aguila; accessed March 2017 from http://www.igvsb.gob.ve/regven.html/

IGVSB, 2017b. Instituto Geográfico de Venezuela Simón Bolívar, Estado MERIDA, Vertice Observatorio; accessed March 2017 from http://www.igvsb.gob.ve/regven.html/

ITRF, 2013. ITRS and WGS84, Last update: 2013-12-11; accessed April 2017 from ftp://itrf.ensg.ign.fr/pub/itrf/WGS84.TXT

ITRF, 2017. Transformation parameters from ITRF2014 to past ITRFs; accessed April 2017 from ftp://itrf.ensg.ign.fr/doc_ITRF/Transfo-ITRF2014_ITRFs.txt

Jekeli, C., 1999. An analysis of vertical deflections derived from high-degree spherical harmonic models. J. Geod 73(1), 10-22.

Kotsakis, C. 2008. Transforming ellipsoidal heights and geoid undulations between different geodetic reference frames. J. Geod. 82, 249–260.

Kudrys, J., 2009. Automatic determination of the deflections of the vertical – first scientific results. Acta Geodyn. Geomater. 6 (3), 233-238.

Kühtreiber, N., 2003. High precision geoid determination of Austria using heterogeneous data. In: Tziavos I.N. (Ed.), *Gravity and Geoid 2002*. Ziti Editions, Thessaloniki, Greece, 144-149.

Mohammed, N.Z., Ghazi, A., Mustafa H.E., 2013. Positional Accuracy Testing of Google Earth. Intern. J. of Multidiscipl. Sci. and Eng. 4(6), 6-9.

Müller, A., Bürki, B., Kahle, H.-G., Hirt, C., Marti, U., 2004. First Results from New High-precision Measurements of Deflections of the Vertical in Switzerland. GGSM 2004 IAG International Symposium Porto, Portugal (ed. C. Jekeli et al.), Springer, Heidelberg, 143-148.

NGA, 2014. World Geodetic System 1984. Its Definition and Relationships with Local Geodetic Systems. National Geospatial-Intelligence Agency (nga) standardization document nga.stnd.0036_1.0.0_WGS84, 2014-07-08

NASA, 2017. Shuttle Radar Topography Mission - U.S. Releases Enhanced Shuttle Land Elevation Data. Available at https://www2.jpl.nasa.gov/srtm/

Pail, R. Goiginger, H., Schuh, W.D., Höck, E., Brockmann, J.M., Fecher, T., Gruber, T., Mayer-Gürr, T., Kusche, J., Jäggi, A., Rieser, 2010. Combined satellite gravity field model GOCO01S derived from GOCE and GRACE. Geophys. Res. Lett. 37(20), L20314.

Pavlis N.K., Holmes, S.A., Kenyon, S.C., Factor, J.K., 2008. An Earth Gravitational Model to Degree 2160: EGM2008, Presented at the 2008 General Assembly of the European Geoscience Union, Vienna, Austria, April 13-18, 2008.

Pavlis N.K., Holmes, S.A., Kenyon, S.C., Factor, J.K., 2012. The development and evaluation of the Earth Gravitational Model 2008 (EGM2008). J Geophys Res – Solid Earth 117:B04406.

Pavlis N.K., Holmes, S.A., Kenyon, S.C., Factor, J.K., 2013. Correction to the development and evaluation of the Earth Gravitational Model 2008 (EGM2008). J Geophys Res – Solid Earth 118(5): 2633-2633.

Potere, D., 2008. Horizontal Positional Accuracy of Google Earth's High-Resolution Imagery Archive, Sensors, 8(12), 7973-7981.

Schack, P., Hirt, C., Hauk, M., Featherstone, W.E., Lyon, T., Guillaume, S., 2018. A high-precision digital astrogeodetic traverse in an area of steep gravity gradients close to the coast of Perth, Western Australia, J. Geod. online first, doi:10.1007/s00190-017-1107-x.

Seeber, G., 2003. Satellite Geodesy, 2nd Edition, de Gruyter, Berlin/New York.

Smith, D.A., Holmes, S.A., Li, X., Guillaume, S., Wang, Y.M., Bürki, B., Roman, D.R., Damiani, T.M., 2013. Confirming regional 1 cm differential geoid accuracy from airborne gravimetry: The geoid slope validation survey of 2011. J. Geod. 87(10-12), 885-907.

Somieski, A.E., Bürki, B., Kahle, H.-G., Marti, U., Hirt, C., Tziavos, I.N., 2007. Determination of Highly-Precise Deflections of the Vertical: Switzerland 2003/2005, Portugal 2004 and Greece 2005, In: Swiss National Report on the Geodetic Activities in the years 2003-2007, presented to the XXIV General Assembly of the IUGG in Perugia, Italy, ISBN 978-3-908440-15-4, Swiss Geodetic Commission, 47-52.

Somieski, A.E., 2008. *Astrogeodetic Geoid and Isostatic Considerations in the North Aegean Sea, Greece*. PhD Thesis, ETH No. 17790, ETH Zurich, Switzerland.

Torge, W., 1985. Geodätische Forschungen in Venezuela; Katalog zur Ausstellung „Forschungs-förderung für Lateinamerika“ der Stiftung Volkswagenwerk.

Torge, W., 2001. Geodesy, 3rd Edition, De Gruyter, Berlin/New York.

Torge, W., Müller, J., 2012. Geodesy. 4th Edition, De Gruyter, Berlin/Boston.

Tóth, G. Völgyesi, L., 2016. Data processing of QDaedalus measurements. Geosciences and Engineering 5(8), 149–166.

Tugluoglo, A., 1971. Über die Empfindlichkeit astronomisch-geodätischer Lotabweichungen gegenüber Dichte-Anomalien des Untergrundes, nebst einer Anwendung auf die Bestimmung der Tiefenstrukturen im Nördlinger Ries. Dissertation. Institut für Theoretische Geodäsie, Universität Bonn.

Van Westrum, D., 2016. GSVS17 - Testing Geoid Models in the Mountains of Colorado, Presentation, available from www.ngs.noaa.gov.

Voigt, C., 2013. Astrogeodätische Lotabweichungen zur Validierung von Schwerefeldmodellen. Deutsche Geodätische Kommission C 702, München.

Wang, B., Tian, L., Wang, Z., et al., 2014. Image and data processing of digital zenith telescope (DZT-1) of China, Chin. Sci. Bull. 59(17), 1984-1991.

Wang, Y.M., Becker, C., Mader, G., Martin, D., Li, X., Jiang, T., Breidenbach, S., Geoghegan, C., Winester, D., Guillaume, S., Bürki, B., 2017. The Geoid Slope Validation Survey 2014 and GRAV-D airborne gravity enhanced geoid comparison results in Iowa. J Geod 91(10),1261-1276.

Wissel, H., 1982. Zur Leistungsfähigkeit von transportablen Zenitkameras bei der Lotabweichungsbestimmung. Wissen. Arb. Fach. Vermessungswesen Univ. Hannover Nr. 107.

Wildermann, E., 1988. Untersuchungen zur lokalen Schwerefeldbestimmung aus heterogenen Daten dargestellt am Beispiel der Geotraverse venezolanische Anden. Wissen. Arb. Fach. Vermessungswesen Univ. Hannover Nr. 155.

Yamazaki, D., Ikeshima, D., Tawatari, R., Yamaguchi, T., O’Loughlin, F., Neal, J.C., Sampson, C.C., Kanae, S., Bates, P.D., 2017. A high accuracy map of global terrain elevations, Geophys. Res. Lett. doi: 10.1002/2017GL072874.